

Article

Mechanical Behavior of Subcutaneous and Visceral Abdominal Adipose Tissue in Patients with Obesity

Chiara Giulia Fontanella ^{1,2,*} , Ilaria Toniolo ^{1,2} , Mirto Foletto ^{2,3,4}, Luca Prevedello ⁴ and Emanuele Luigi Carniel ^{1,2} 

- ¹ Department of Industrial Engineering, University of Padova, 35131 Padova, Italy
² Centre for Mechanics of Biological Materials, University of Padova, 35131 Padova, Italy
³ IFSO Bariatric Center of Excellence, Policlinico Universitario (Azienda Ospedaliera di Padova), 35131 Padova, Italy
⁴ Department of Surgery, Oncology and Gastroenterology, University of Padova, 35131 Padova, Italy
* Correspondence: chiara.giulia.fontanella@unipd.it; Tel.: +39-049-827-6754

Abstract: The mechanical characterization of adipose tissues is important for various medical purposes, including plastic surgery and biomechanical applications, such as computational human body models for the simulation of surgical procedures or injury prediction, for example, in the evaluation of vehicle crashworthiness. In this context, the measurement of human subcutaneous adipose tissue (SAT) and visceral adipose tissue (VAT) mechanical properties in relation to subject characteristics may be really relevant. The aim of this work was to properly characterize the mechanical response of adipose tissues in patients with obesity. Then, the data were exploited to develop a reliable finite element model of the adipose tissues characterized by a constitutive material model that accounted for nonlinear elasticity and time dependence. Mechanical tests have been performed on both SAT and VAT specimens, which have been harvested from patients with severe obesity during standard laparoscopic sleeve gastrectomy intervention. The experimental campaign included indentation tests, which permitted us to obtain the initial/final indentation stiffnesses for each specimen. Statistical results revealed a higher statistical stiffness in SAT than in VAT, with an initial/final indentation stiffness of 1.65 (SD ± 0.29) N/30.30 (SD ± 20) N compared to 1.29 (SD ± 0.30) N/21.00 (SD ± 16) N. Moreover, the results showed that gender, BMI, and age did not significantly affect the stiffness. The experimental results were used in the identification of the constitutive parameters to be inserted in the constitutive material model. Such constitutive characterization of VAT and SAT mechanics can be the starting point for the future development of more accurate computational models of the human adipose tissue and, in general, of the human body for the optimization of numerous medical and biomechanical procedures and applications.

Keywords: abdominal visceral adipose tissue; subcutaneous adipose tissue; biomechanical behavior; obesity; indentation tests; constitutive modelling; finite element modelling



Citation: Fontanella, C.G.; Toniolo, I.; Foletto, M.; Prevedello, L.; Carniel, E.L. Mechanical Behavior of Subcutaneous and Visceral Abdominal Adipose Tissue in Patients with Obesity. *Processes* **2022**, *10*, 1798. <https://doi.org/10.3390/pr10091798>

Academic Editor: Chi-Fai Chau

Received: 3 August 2022

Accepted: 3 September 2022

Published: 7 September 2022

Publisher's Note: MDPI stays neutral with regard to jurisdictional claims in published maps and institutional affiliations.



Copyright: © 2022 by the authors. Licensee MDPI, Basel, Switzerland. This article is an open access article distributed under the terms and conditions of the Creative Commons Attribution (CC BY) license (<https://creativecommons.org/licenses/by/4.0/>).

1. Introduction

The mechanical analysis of adipose tissue (AT) is essential for its role in cosmetics, wounds, and plastic surgery related to trauma, burn injuries, cancer resections, and congenital deformities [1]. Moreover, the experimental characterization of the mechanical response of adipose tissue is necessary for a computational model definition, identification, and validation. The methods of computational biomechanics lead to structural modeling tools that allow mechano-physical investigations, providing relevant information for the optimization of surgical procedures' design, equipment, prosthetic devices, and for the assessments related to reliability. Moreover, finite element (FE) models of the abdominal region allow for the investigation of mechanical functionality, with regard to interaction phenomena with external systems (e.g., the computational simulation of vehicular crashes) [2–4].

Abdominal adipose tissue differs in visceral (VAT) and subcutaneous (SAT) adipose tissue (Figure 1a). There are molecular, cellular, anatomical, physiological, clinical, and prognostic differences between SAT and VAT [5–7]. VAT is located inside the abdominal cavity, packed among the organs, and it is composed of several adipose depots, including mesenteric and perirenal depots, and epididymal white adipose tissue. SAT accounts for most adipose tissue, approximately 85% of the adipose tissue of the human body, and it is located under the skin. AT consists of a lobular type of white adipose tissue. Adipocytes are arranged into lobules with a diameter of approximately 1 mm and separated from each other by interlobular septa. Interlobular septa are predominantly type I collagen fiber networks and are several mm in length, with a diameter ranging between 10 nm and 30 μm [8]. The dimension of lobules and the thickness of interlobular septa change among fat tissues [9–12], with a consequent differentiation of mechanical properties and roles [13].

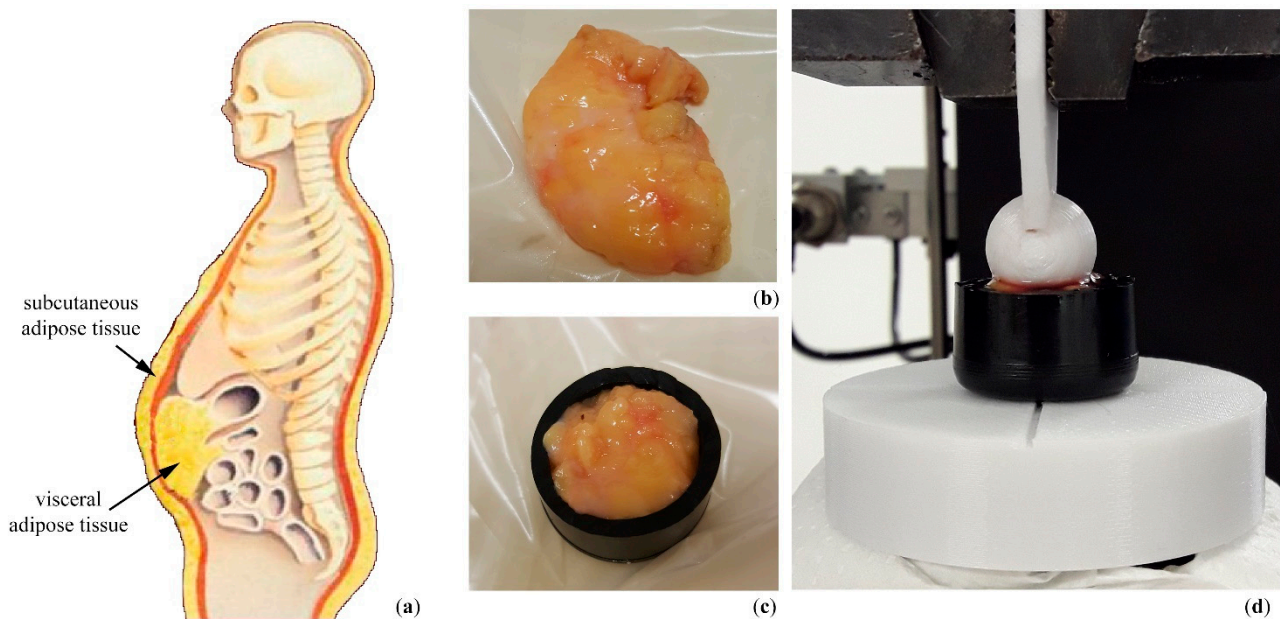


Figure 1. (a) Identification of subcutaneous and visceral adipose tissue. (b) Tissue portions of SAT and VAT were harvested during the laparoscopic sleeve gastrectomy intervention and (c) cylindrical specimens of 20 mm diameter were cut. (d) Indentation tests involved the use of an indenter spherical in shape characterized by a 10-mm diameter.

Obesity is a complex disease involving an excessive amount of AT, making it a major risk factor for diabetes and cardiovascular disease. Subjects with obesity vary in body fat distribution, metabolic profile, and degree of associated cardiovascular and metabolic risk [14–16]. Excess in both VAT and SAT contribute to obesity, even if VAT and SAT differ in structural composition, metabolic activity, functional significance, and mechanical behavior [17,18].

Various types of mechanical experiments were performed on adipose tissue, using animal and human models [8,19,20]. Mechanical characterization has been performed by confined and unconfined compression tests, indentation tests, and shear or tensile tests [1,8,21–24]. These experiments were adopted to obtain Young’s modulus and shear modulus in dependence on loading protocol and specimen source. Rheological experiments were performed to measure the viscoelastic behavior of the tissues [25]. Experimental data highlight the nonlinear stress-strain response and time-dependent behavior of adipose tissue. In the literature, constitutive analysis has been performed using hyperelastic or viscoelastic models [8,26].

Despite the several experimental campaigns proposed in the literature, poor data were provided regarding the characterization of human VAT and SAT, with a focus on how obesity affects the mechanical response of the tissues [27]. Here, the reported activities were

aimed at providing a description of human VAT and SAT properties, with a specific focus on mechanical behavior. Indentation tests on specimens obtained from subjects with severe obesity make it possible to discriminate between VAT and SAT mechanics and to evaluate the influence of subject characteristics, such as gender, BMI, and age, on the mechanical response. The choice fell on the indentation test because of the structural organization of the adipose tissue and its laxity does not allow for easy access to samples for tensile tests. Moreover, AT mechanical functions consist of supporting and protecting, hence the mechanical tests, which mostly preserve the integrity of the tissue and mimic its mechanical action, are indentation and compression tests [19,24,28]. A visco-hyperelastic constitutive model has been formulated to describe the mechanical behavior, and constitutive parameters have been identified by the inverse finite element analysis (FEA) of experimental tests.

The innovations introduced by this work regarding: (i) the mechanical characterization of human VAT and SAT through experimental tests; (ii) the influence of the subject's characteristics on AT mechanics; and (iii) the development of FE models suitable for interpreting their mechanical responses. These data can be used to improve FE models of the human abdominal region, providing tools for computational simulations in the medical and engineering areas.

2. Materials and Methods

2.1. Specimen Preparation

VAT and SAT specimens (Figure 1b) from bariatric patients of Padova University Hospital were used in the experimental campaign from January 2018 to January 2020. A total of 19 patients affected by severe obesity and scheduled for laparoscopic sleeve gastrectomy (LSG) were enrolled (gender 5M vs. 14 F; age 46 ± 11 , BMI 46 ± 5 kg/m²). All patients gave informed consent. The local Ethical Committee approved experimentations on adipose tissues (Padova Healthcare Ethics Committees, Protocol N° 2892P). The criteria reported in the international bariatric surgery guidelines were respected, and further restrictions were added, as follows [28,29]: the range of BMI had to be comprehended between 35 and 60 kg/m², no contraindications to LSG (i.e., the presence of great hiatal hernia or severe gastroesophageal reflux disease), and primary bariatric surgery. LSG respected the standard surgical technique [29–31]. During the operation, approximately volumes of 2 cm³ of AT in the visceral and subcutaneous regions were harvested. Each sample was gently cleaned with a cold physiological solution to eliminate tissue debris and blood remains. Subsequently, samples were stored frozen at -20 °C in sealed vials and thawed before testing [8,20,32]. These storage methods do not alter the mechanical response of soft biological tissues, as confirmed by previous experiences with human adipose tissues [20,32]. All the subsequent mechanical tests were performed within three hours of defrosting at room temperature. During preparation and testing, samples were continuously moistened with a physiological solution at room temperature.

2.2. Mechanical Testing

Cylindrical samples were obtained by a cutting punch of 20 mm in diameter and a digital caliper was used to measure sample thickness (mean thickness 9.1 ± 2.3 mm). Each sample was placed in a cylindrical container (Figure 1c) and indentation tests with a spherical indenter (10 mm diameter) were conducted. To compare the results of the different samples, indentation strain was computed as the ratio between the indenter displacement and the initial thickness of each sample. A Galdabini material testing machine (Galdabini Cesare SpA, Varese, Italy) (Figure 1d) was used to apply the loading action [33]. Based on a preliminary evaluation of tissue stiffness, a load cell with a capacity of 100 N and an accuracy of $\pm 0.1\%$ was adopted.

Before testing, each sample was preconditioned by applying 10 loading-unloading cycles with indentation strain ranging between 0 and 20% at a 10%/s strain rate. Indentation tests were developed using a ramp-hold stress relaxation test [33,34]: five consecutive ramps of 15% indentation strain at 3000%/s strain rate followed by 300 s holds [35] (Figure 2). The

duration of the resting period was assumed to allow the almost complete development of relaxation phenomena, taking into consideration the typical values of relaxation times of soft biological tissues [35–37].

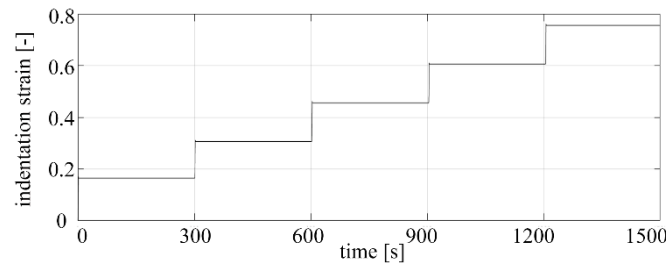


Figure 2. Experimental protocol: the ramp-hold stress relaxation tests for indentation tests.

2.3. Data Elaboration

The analysis of each indentation test allowed for the achievement of the mechanical response of the tissues at equilibrium and the viscoelastic behavior, which are necessary for the definition of the constitutive models. The equilibrium behavior occurs at the end of the relaxation stages or during a continuous straining test if the strain rate is sufficiently low, when all the time-dependent micro-structural rearrangement phenomena can completely develop [38,39]. Consequently, force and indentation strain data at the end of the holding stages led to almost-equilibrium force-indentation strain curves. On the other hand, the analysis of force-time results during the constant strain stages led to force relaxation curves [33]. Force-relaxation data were processed to identify the drop of normalized force with time. The normalized force is defined as the ratio of the force at the current time and the peak force at the beginning of each relaxation stage.

Concerning each test, the force-indentation strain curve at equilibrium required post-processing operations aiming to exclude straining data bias due to surface irregularity of the samples and indenter adjustment along the loading direction. A 0.1 N cutting force value, as a threshold, was assumed, by considering the load-cell sensitivity. Force-indentation strain at equilibrium and normalized force-time curves were fitted in Matlab (MATLAB R2019b, The MathWorks Inc., Natick, MA, USA) by the following exponential formulations:

$$F(\varepsilon) = \frac{c}{\alpha} [\exp(\alpha\varepsilon) - 1] \quad (1)$$

$$\bar{F}(t) = 1 - \gamma_1 \left[1 - \exp\left(-\frac{t}{\tau_1}\right) \right] - \gamma_2 \left[1 - \exp\left(-\frac{t}{\tau_2}\right) \right] \quad (2)$$

where F is the equilibrium force and \bar{F} is the normalized force, ε is the indentation strain, t is the time, while c , α , and γ_1 , γ_2 , τ_1 , and τ_2 are parameters sets that interpret the nonlinear elastic behavior and the viscoelastic response of the tissue [33].

For each force-indentation strain curve at equilibrium, the initial and the final indentation stiffnesses were calculated. In detail, the initial indentation stiffness was defined as the slope of the curve in the initial phase (0 ÷ 10% indentation strain range), while the final indentation stiffness was defined as the slope in the quasi-linear region (40% ÷ 50% indentation strain range). Finally, the statistical analysis of force-strain and normalized force-time curves from all the samples led to an average data about SAT and VAT tissues mechanics.

2.4. Constitutive Analysis

Aiming to provide an effective characterization of VAT and SAT mechanical behavior, tissue mechanics has to be characterized in the framework of a constitutive formulation. The constitutive model is a mathematical tool that defines the general stress-strain behavior of the material. The mathematical formulation involves constitutive parameters, which characterize the mechanical properties of the tissue. Inverse analysis techniques of experi-

mental activities allow the identification of such parameters and require the development of computational models mimicking the testing procedures.

Results showed the nonlinearity and the time-dependence in the mechanical responses of VAT and SAT, leading to a constitutive model that accounted for visco-hyperelasticity [39]. The Helmholtz free energy function ψ was reported in terms of the right Cauchy-Green strain tensor C and viscous variables q^i . C specifies the instantaneous strain condition, while q^i defines viscous relaxation and dissipation phenomena [40]:

$$\psi(C, q^i) = W^0(C) - \sum_{i=1}^n \int_0^t \frac{1}{2} q^i(s) : \dot{C} ds \quad (3)$$

where W^∞ is the hyperelastic potential which delineates mechanical response at the equilibrium, while the integral defines the viscous contribution by means of n viscous branches. An Ogden formulation was assumed to define the equilibrium response of VAT and SAT tissues:

$$W^\infty(\tilde{\lambda}_1, \tilde{\lambda}_2, \tilde{\lambda}_3) = \frac{2\mu}{\alpha^2} [\tilde{\lambda}_1^\alpha + \tilde{\lambda}_2^\alpha + \tilde{\lambda}_3^\alpha - 3] + \frac{1}{D} (J - 1)^2 \quad (4)$$

where $\tilde{\lambda}_i$ are the iso-volumetric principal stretches and μ, α, D are hyperelastic parameters. The parameter μ defines the initial shear stiffness, such as $G_0 = \mu$. The parameter α describes the nonlinearity of tissue elasticity, as the increase in elastic stiffness with stretching phenomena. J is the deformation Jacobian, while the parameter D is the initial volumetric compliance. To describe the evolution of viscous variables over time, integral formulations were adopted. They depend on stress-strain history and viscous parameters, as relative stiffnesses γ^∞, γ^i and relaxation times τ^i [40,41]:

$$q^i(t) = \frac{\gamma^i}{\gamma^\infty \tau^i} \int_0^t \exp\left(-\frac{t-s}{\tau^i}\right) \left(\frac{2\partial W^\infty(C)}{\partial C}\right) ds \quad (5)$$

The FE models were developed in order to simulate the experimental lab test. Hence, the spherical indenter (10-mm diameter) and the cylindrical shaped sample (20 mm diameter, 9.1 mm height) were designed in FE preprocessing software Abaqus CAE 2019 (Dassault Systèmes Simulia Corp., Providence, RI, USA). The indenter was assumed to be a rigid body (the deformation induced in the indenter by contact with the tissue sample is meaningless), while a frictionless contact was imposed to describe the interface between the indenter and the tissues. The discretization of finite elements consisted of 8-node hexahedral elements. A sensitivity analysis of the mesh discretization was performed by varying the element size and comparing the results. The best compromise between results accuracy and computational burden was found by imposing an average mesh seed of 0.8 mm, which led to a 28,000-node model. The simulations consisted of an indentation that reached 50% deformation, with a strain rate of 3000%/s. The relaxation response was considered after 300 s of resting. The general-purpose FE software Abaqus Standard 2019 was the FE solver.

The numerical simulations evaluated both the equilibrium force-indentation strain and force relaxation conditions. The adipose tissues were described with the visco-hyperelastic constitutive model reported in the previous sections.

The identification of the constitutive parameters was performed by the inverse FEA of experimental activities. In detail, the minimization of a cost function consisting of the difference between the experimental data and the computational results was achieved in order to obtain the optimal constitutive parameters. In the first place, the hyperelastic parameters were set by only considering the data related to the force-indentation strain response at equilibrium. Subsequently, the parameters related to the viscosity were extracted from the analysis of the force relaxation. The viscous branches assumed where to have the best compromise between the number of parameters and the correct interpretation of the trend of the experimental data.

2.5. Statistical Analysis

Experimental data were reported as mean (\pm standard deviation) according to the data distribution. Statistical analyses were performed on the initial and the final indentation stiffnesses. These values were grouped by tissues and by subject characteristics. The distribution of the variables was evaluated with the Shapiro–Wilk test, and then differences among groups were evaluated using a 2-sample *t*-test. A *p*-value lower than 0.05 was considered significant. All analyses were performed with the statistical software Minitab 20 (Minitab, 2020).

3. Results

Mechanical tests were performed on VAT and SAT tissues from patients with severe obesity (Figure 3a). The equilibrium response was obtained for each indentation test considering the force and indentation strain data at the end of the holding stages (Figure 3b), while the normalized force-time curves were obtained considering the holding stage of each ramp (Figure 3c).

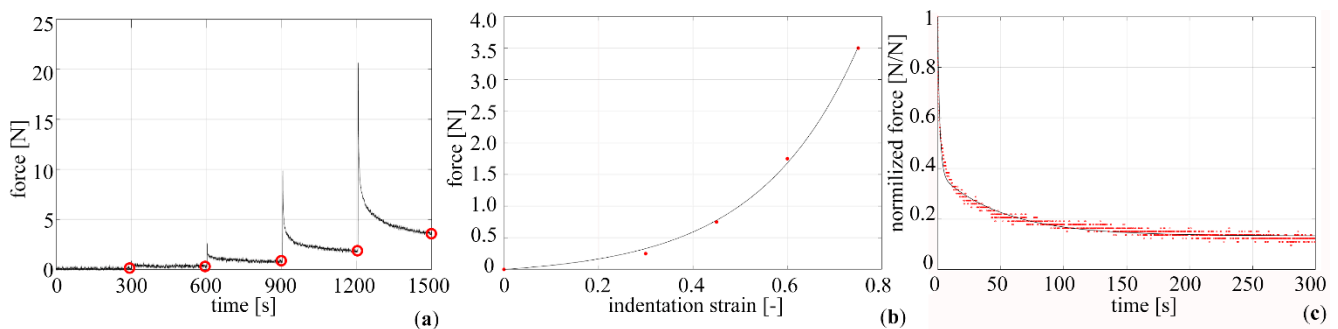


Figure 3. (a) Representative force-time output of a VAT specimen with highlighted equilibrium force (red circles). Elaboration of experimental data: comparison of experimental data (red circle) and fitted results (continuous line) for (b) force-indentation strain at equilibrium and (c) normalized force-time.

The processing of experimental data led to statistical distributions of the force-indentation strain at equilibrium and the normalized force-time curves, by the mean and standard error of the mean (SD) (Figure 4), aiming to highlight the nonlinear stiffening with strain and the viscoelastic behavior of both SAT and VAT. The force relaxation curves showed the micro-structural rearrangement phenomena, due to liquid component flux and fiber alignment. The equilibrium force-strain curves were reported in relation to BMI, age, and gender (Figure 5). The corresponding force relaxation curves were not reported, because no significant differences were observed among groups.

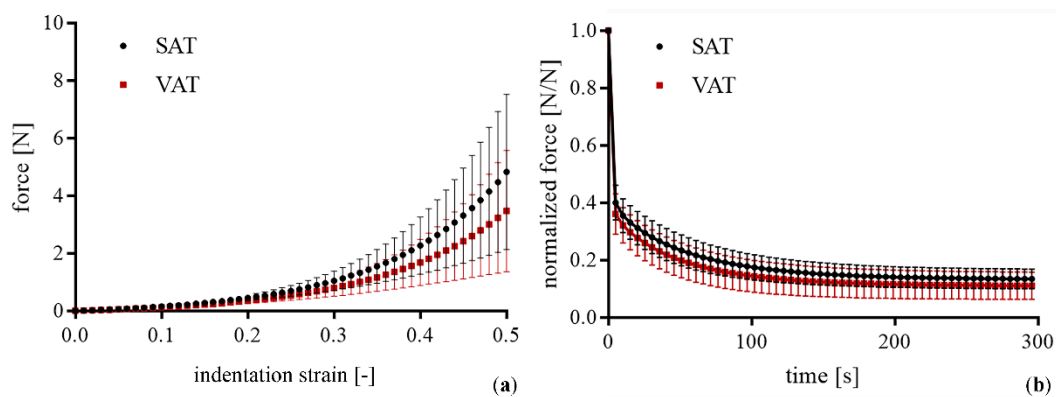


Figure 4. Comparison of mean \pm SD curves from indentation tests performed on SAT and VAT specimens: (a) equilibrium stress-indentation strain data and (b) normalized stress-time results.

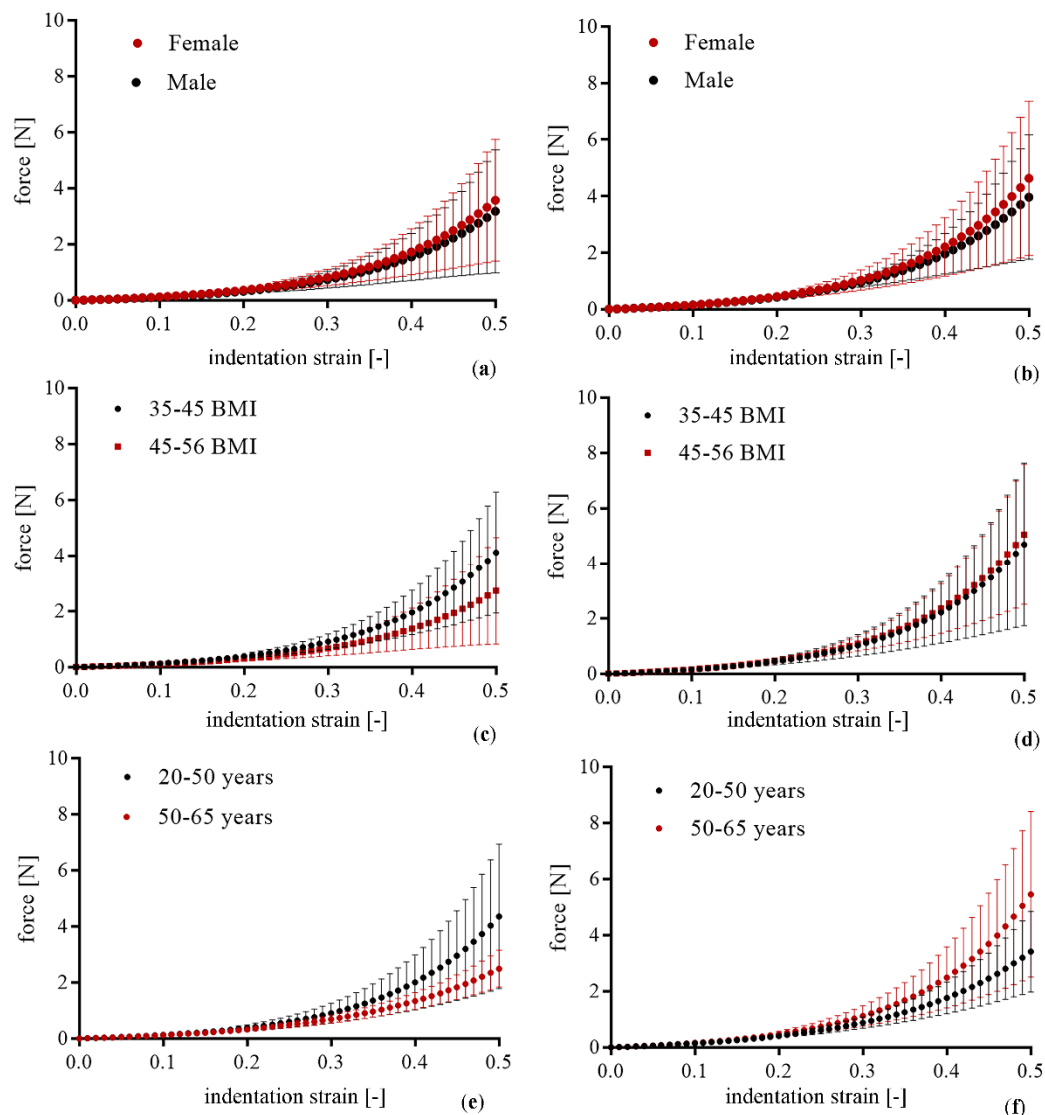


Figure 5. Force vs. indentation strain at equilibrium: tests performed on (a,c,e) VAT and (b,d,f) SAT specimens, and divided into (a,b) male/female subjects, (c,d) subjects with different BMI, and (e,f) subjects with different ages (mean \pm SD).

For each test, the initial and the final indentation stiffnesses of force-indentation strain curves at equilibrium were determined. A comparison between VAT and SAT showed a statistical difference for the initial indentation stiffness (Table 1). No statistical differences were found when the VAT/SAT mechanical response was considered in patients grouped by gender, age (<50 vs. >50 years), and obesity severity (BMI < 45 vs. >45 Kg/m²) (Table 2). The normalized force completely relaxed in \sim 300 s and followed a two-exponential course. There were no significant differences between the viscoelastic constants of VAT and SAT.

Table 1. Initial indentation stiffness and final indentation stiffness for VAT and SAT specimens.

	VAT	SAT	<i>p</i> -Value
initial indentation stiffness [N]	1.29 (\pm 0.30)	1.65 (\pm 0.29)	0.003
final indentation stiffness [N]	21.00 (\pm 16)	30.30 (\pm 20)	0.194

p-values less than 0.05 were considered statistically significant and bolded.

Table 2. Initial indentation stiffness and final indentation stiffness for VAT and SAT in relation to gender, BMI, and age.

	VAT	SAT	<i>p</i> -Value
initial indentation stiffness [N]			
Male vs. Female	1.32 (± 0.31) vs. 1.18 (± 0.27) ^a	1.63 (± 0.15) vs. 1.65 (± 0.32) ^b	^a 0.436 ^b 0.909
Age	1.31 (± 0.30) vs.	1.54 (± 0.24) vs.	^a 0.690
<50 vs. >50 years	1.25 (± 0.30) ^a	1.69 (± 0.30) ^b	^b 0.384
BMI	1.42 (± 0.30) vs.	1.56 (± 0.34) vs.	^a 0.067
<45 vs. >45 Kg/m²	1.14 (± 0.24) ^a	1.75 (± 0.17) ^b	^b 0.252
final indentation stiffness [N]			
Male vs. Female	21.60 (± 16.60) vs. 19.10 (± 16.10) ^a	28.60 (± 20) vs. 35.90 (± 25) ^b	^a 0.801 ^b 0.617
Age	26.10 (± 19.10) vs.	19.10 (± 10.30) vs.	^a 0.132
<50 vs. >50 years	13.21 (± 4.50) ^a	35.32 (± 22.91) ^b	^b 0.211
BMI	25.40 (± 17.11) vs.	28.51 (± 24.32) vs.	^a 0.268
<45 vs. >45 Kg/m²	15.90 (± 14.30) ^a	32.31 (± 18.20) ^b	^b 0.759

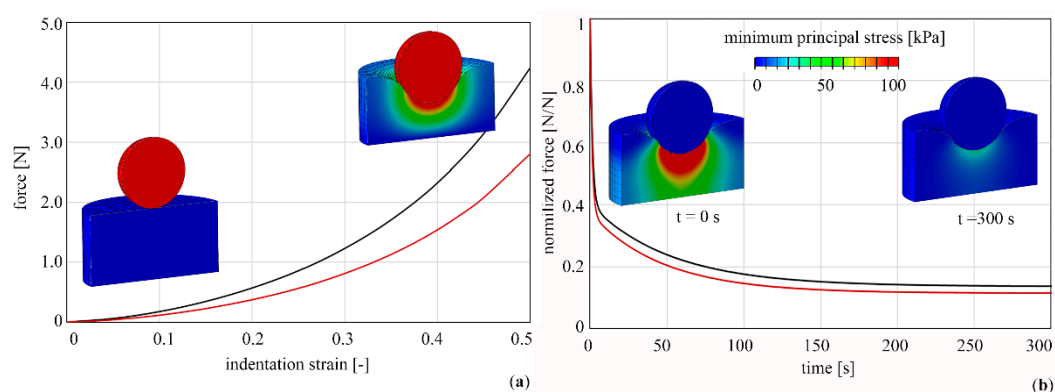
p-values less than 0.05 were considered statistically significant and bolded; (a,b) male/female subjects.

The mechanical responses of VAT and SAT showed nonlinear elasticity and time-dependent behaviors. The visco-hyperelastic constitutive model with two viscous branches was considered for interpreting the mechanical response of the adipose tissues, with the final aim of developing computational models. The discrepancies between the average experimental data and the results from the computational model, with the associated constitutive parameters, were evaluated using the mean absolute percentage error in terms of forces. For SAT and VAT, the values of discrepancy at equilibrium were 3.9% and 4.2%, while for the force relaxation responses were 8.1% and 8.9%, respectively. Constitutive parameters and computational results were reported in Table 3 and Figure 6, respectively.

Table 3. Visco-hyperelastic constitutive parameters for VAT and SAT.

	μ (kPa)	α	D (kPa ⁻¹)	γ_1	γ_2	τ_1 (s)	τ_2 (s)
VAT	12.55	7.23	64.66	0.63	0.27	1.21	47.48
SAT	17.50	10.11	65.66	0.60	0.26	1.41	52.63

The contour of minimum principal stress was reported for the force relaxation analysis of VAT samples, showing the capability of the tissue to relax stresses during time through microstructural rearrangement phenomena.

**Figure 6.** Computational analysis of indentation tests for VAT (red lines) and SAT (black lines). (a) Equilibrium stress-indentation strain with contours of displacement magnitude in unstrained and strained configurations. (b) Normalized stress-time responses of indentation tests with contours of minimum principal stress at time $t = 0$ s and $t = 300$ s.

4. Discussion

Visceral and abdominal subcutaneous adipose tissues contribute to obesity but may have different metabolic risk profiles. VAT is also associated with prevalent diabetes, metabolic syndrome, hepatic steatosis, and aortic plaque [18,42,43]. Previous experiments did not characterize SAT and VAT mechanics, with particular regard to overweight and obesity conditions. Here, the reported experiments highlight that there are mechanical differences in stiffness between SAT and VAT tissues belonging to patients with severe obesity. Computational investigations and the identified parameters confirm this observation, showing major stiffness for SAT compared to VAT. With regard to the micro-structural configuration, human SAT adipocytes demonstrate increased adipocyte hypertrophy relative to VAT adipocytes, with a consequent cellular stiffening [23]. Moreover, in the extracellular matrix, collagen IV and laminin are higher in VAT than in SAT, while collagen I and matrix stiffness of SAT are higher in comparison to VAT [44]. These microstructural characteristics may explain our mechanical results, with a SAT stiffness larger than the VAT one.

A similar mechanical response is reported for both abdominal adipose tissues in male and female subjects, while the influence of ageing determines different mechanical responses for both SAT and VAT. On the contrary, the increase in BMI causes a decrease in stiffness in both visceral and subcutaneous adipose tissues, probably due to uncontrolled extracellular matrix (ECM) production [45]. Patients' BMI ranged from the condition of severe obesity to the beginning of super obesity [46]. Patients were not affected by pathologies, other than obesity, which significantly contributes to altering AT mechanics. The micro-structural rearrangement processes produce stress drop effects and determine the amplitude and duration of relaxation phenomena. The same typologies of micro-structural rearrangement processes characterize adipose tissues from different regions, regardless of the specific loading direction.

In the literature, few studies report the comparison between VAT and SAT mechanics. Alkouli et al., 2013, evaluated SAT and VAT mechanical responses using tensile tests, observing major stiffness in tensile loading for VAT compared to SAT [21]. However, some differences can be found with respect to our study: the mean BMI ($30.2 \pm 6.4 \text{ kg/m}^2$ and $28.9 \pm 6 \text{ kg/m}^2$) was lower than in our study, and the specimens were mainly obtained from human cadavers. Rheological methods were used to determine the viscoelastic properties of diabetic and nondiabetic human VAT and SAT by Juliar et al. 2020. They observed VAT stiffness being lower than SAT stiffness, as reported in our study. Similar to our results, no statistical differences were found considering gender, BMI, age, and diabetic conditions with regard to both VAT and SAT [23].

The time-dependent and nonlinear elastic behavior of AT is confirmed by other studies. SAT mechanical properties have been evaluated using compression and shear tests by [19,24]. They confirmed the time-dependent response of the tissue and proposed a quasilinear viscoelastic model to describe the mechanical response. In their studies, the mechanical response of porcine AT was found to be stiffer than human ones, pointing out the relevance of analyzing the mechanical response of AT from the human model. The viscoelastic mechanical properties of the human SAT have been studied by [47], using a different experimental test. The abdominal adipose tissue samples belonged to an old female patient who was subjected to deep inferior epigastric perforator (DIEP) flap surgery. The experimental tests performed on these specimens consisted of unconfined uniaxial compression, considering a resting period that permits analyzing the relaxation phenomena. The mechanical response was described with different constitutive models, which were able to interpret the nonlinearity of the stress-strain curve and the time-dependent behavior. Similarly, Sommer et al. (2013) analyzed human SAT with biaxial tensile and triaxial shear tests [1]. Adipose samples were obtained from nine patients subjected to DIEP flap surgery. The results suggest that human abdominal adipose tissues can be characterized as a nonlinear, anisotropic, and viscoelastic material. Although the mechanical behavior is similar, it is difficult to compare these results with those of the reported activities because the experimental test and the loading conditions, such as the strain rate, are different.

Furthermore, the tests report the results of patients who underwent DIEP flap surgery and not a collection of data from patients with obesity. An interesting study has been proposed by Unanumo et al. (2022), which analyzes the influence of bariatric surgery on the biomechanical properties of AT in human and animal models. This study reports only tensile tests, which cannot be compared to our results, however, they confirm the influence of both obesity and bariatric surgery on the AT mechanical response.

In the literature, the biomechanical properties of abdominal adipose tissues have been investigated for plastic and reconstructive surgery to support the surgeon's planning and to improve surgical outcomes [1]. The current methods for surgery involve artificial material filling or autologous tissue transplantation. Mechanical data here reported may be relevant in fat graft injection for surgical reconstruction of soft-tissue deficits, also considering the intra- and inter-subjects' variability. More recently, FE models and simulations have been adopted for the investigation of the risk of abdominal and lower extremity injuries during vehicular crashes. Adipose tissues have an important role in the transfer of impact loads and in protecting organs from related injuries [3,48]. These models can be used to explore the large-scale responses of tissues and organs in clinical and pathophysiological research. Data on the mechanical response of abdominal adipose tissues can improve the development of such FE models.

In conclusion, this work permits the analyzation of the differences in VAT and SAT belonging to patients with severe obesity by performing experimental indentation tests. Furthermore, the experimental results were exploited for identifying the constitutive parameters of a nonlinear visco-hyperelastic material model. This mechanical characterization could be very useful for the development of reliable computation models of the abdomen able to properly predict the outcomes of medical and biomechanical applications, such as in the simulation of surgical procedures or injury prediction, e.g., in the evaluation of vehicle crashworthiness. Nevertheless, the study has some limitations. First, the analysis has been conducted in a small sample size and it would be interesting to confirm our observations in a larger population. Second, the specimens obtained from the surgery were really soft, and the irregularity of the surfaces did not allow us to obtain a geometric shape for the development of uniaxial compression or tensile tests. Consequently, the developed experiments assumed indentation conditions only. Future research directions could include the analysis of AT considering further loading conditions, such as uni- and bi-axial tests or shear/torsional tests.

5. Conclusions

Here, the reported activities aimed at characterizing human VAT and SAT mechanics, with particular attention to the population with severe obesity. Constitutive analysis has been proposed to implement computational models of the abdominal region. Computational tools can be adopted in the medical areas, e.g., plastic surgery, or the engineering areas, e.g., for the identification of human body responses during crashes. Experimental data allows us to obtain information about the influence of subject characteristics, pointing out intra- and inter-subject variability, for the development of subject-specific FE models.

Author Contributions: Conceptualization, C.G.F., E.L.C. and M.F.; methodology, C.G.F.; validation, C.G.F. and E.L.C.; formal analysis, C.G.F.; investigation, C.G.F. and M.F.; resources, L.P. and M.F.; data curation, C.G.F., I.T. and E.L.C.; writing—original draft preparation, C.G.F. and E.L.C. writing—review and editing, C.G.F., I.T., M.F. and E.L.C.; visualization, C.G.F. and E.L.C.; supervision, M.F. and E.L.C.; funding acquisition, E.L.C. All authors have read and agreed to the published version of the manuscript.

Funding: This research was funded by the Italian Ministry of University and Research: FIS2019_03221 "CECOMES—CEntro di studi sperimentali e COmputazionali per la ModElliStica applicata alla chirurgia".

Institutional Review Board Statement: The study was conducted according to the guidelines of the Declaration of Helsinki, and approved by the Padova Healthcare Ethics Committees, protocol no. 2892P.

Informed Consent Statement: Informed consent was obtained from all subjects involved in the study.

Data Availability Statement: The data presented in this study are available on request from the corresponding author.

Conflicts of Interest: The authors declare no conflict of interest. The funders had no role in the design of the study; in the collection, analyses, or interpretation of data; in the writing of the manuscript, or in the decision to publish the results.

References

- Sommer, G.; Eder, M.; Kovacs, L.; Pathak, H.; Bonitz, L.; Mueller, C.; Regitnig, P.; Holzapfel, G.A. Multiaxial Mechanical Properties and Constitutive Modeling of Human Adipose Tissue: A Basis for Preoperative Simulations in Plastic and Reconstructive Surgery. *Acta Biomater.* **2013**, *9*, 9036–9048. [[CrossRef](#)] [[PubMed](#)]
- Carniel, E.L.; Toniolo, I.; Fontanella, C.G. Computational Biomechanics: In-Silico Tools for the Investigation of Surgical Procedures and Devices. *Bioengineering* **2020**, *7*, 48. [[CrossRef](#)]
- Naseri, H.; Iraeus, J.; Johansson, H. The Effect of Adipose Tissue Material Properties on the Lap Belt-Pelvis Interaction: A Global Sensitivity Analysis. *J. Mech. Behav. Biomed. Mater.* **2020**, *107*, 103739. [[CrossRef](#)]
- Gierczycka, D.; Rycman, A.; Cronin, D. Importance of Passive Muscle, Skin, and Adipose Tissue Mechanical Properties on Head and Neck Response in Rear Impacts Assessed with a Finite Element Model. *Traffic. Inj. Prev.* **2021**, *22*, 407–412. [[CrossRef](#)]
- Fox, C.S.; Massaro, J.M.; Hoffmann, U.; Pou, K.M.; Maurovich-Horvat, P.; Liu, C.-Y.; Vasan, R.S.; Murabito, J.M.; Meigs, J.B.; Cupples, L.A.; et al. Abdominal Visceral and Subcutaneous Adipose Tissue Compartments: Association with Metabolic Risk Factors in the Framingham Heart Study. *Circulation* **2007**, *116*, 39–48. [[CrossRef](#)]
- Illouz, F.; Roulier, V.; Rod, A.; Gallois, Y.; Pellé, C.-P.; Aubé, C.; Rohmer, V.; Ritz, P.; Ducluzeau, P.H. Distribution of Adipose Tissue: Quantification and Relationship with Hepatic Steatosis and Vascular Profiles of Type 2 Diabetic Patients with Metabolic Syndrome. *Diabetes Metab.* **2008**, *34*, 68–74. [[CrossRef](#)] [[PubMed](#)]
- Kim, Y.J.; Park, J.W.; Kim, J.W.; Park, C.-S.; Gonzalez, J.P.S.; Lee, S.H.; Kim, K.G.; Oh, J.H. Computerized Automated Quantification of Subcutaneous and Visceral Adipose Tissue From Computed Tomography Scans: Development and Validation Study. *JMIR Med. Inform.* **2016**, *4*, e2. [[CrossRef](#)] [[PubMed](#)]
- Sun, Z.; Gepner, B.D.; Cottler, P.S.; Lee, S.H.; Kerrigan, J.R. In Vitro Mechanical Characterization and Modeling of Subcutaneous Adipose Tissue: A Comprehensive Review. *J. Biomech. Eng.* **2021**, *143*, 070803. [[CrossRef](#)] [[PubMed](#)]
- Macchi, V.; Porzionato, A.; Sarasin, G.; Petrelli, L.; Guidolin, D.; Rossato, M.; Fontanella, C.G.; Natali, A.; De Caro, R. The Infrapatellar Adipose Body: A Histotopographic Study. *Cells Tissues Organs* **2016**, *201*, 220–231. [[CrossRef](#)]
- Natali, A.N.; Fontanella, C.G.; Carniel, E.L. A Numerical Model for Investigating the Mechanics of Calcaneal Fat Pad Region. *J. Mech. Behav. Biomed. Mater.* **2012**, *5*, 216–223. [[CrossRef](#)]
- Friego, A.; Costantini, M.; Fontanella, C.G.; Salvador, R.; Merigliano, S.; Carniel, E.L. A Procedure for the Automatic Analysis of High-Resolution Manometry Data to Support the Clinical Diagnosis of Esophageal Motility Disorders. *IEEE Trans. Biomed. Eng.* **2018**, *65*, 1476–1485. [[CrossRef](#)] [[PubMed](#)]
- Fontanella, C.G.; Macchi, V.; Carniel, E.L.; Friego, A.; Porzionato, A.; Picardi, E.E.E.; Favero, M.; Ruggieri, P.; de Caro, R.; Natali, A.N. Biomechanical Behavior of Hoffa's Fat Pad in Healthy and Osteoarthritic Conditions: Histological and Mechanical Investigations. *Australas Phys. Eng. Sci. Med.* **2018**, *41*, 657–667. [[CrossRef](#)] [[PubMed](#)]
- Dragoo, J.L.; Shapiro, S.A.; Bradsell, H.; Frank, R.M. The Essential Roles of Human Adipose Tissue: Metabolic, Thermoregulatory, Cellular, and Paracrine Effects. *J. Cartil. Jt. Preserv.* **2021**, *1*, 100023. [[CrossRef](#)]
- Ahrens, W.; Pigeot, I.; Pohlabeln, H.; De Henauw, S.; Lissner, L.; Molnár, D.; Moreno, L.A.; Tornaritis, M.; Veidebaum, T.; Siani, A. Prevalence of Overweight and Obesity in European Children below the Age of 10. *Int. J. Obes.* **2014**, *38* (Suppl. 2), S99–S107. [[CrossRef](#)]
- Bahia, L.; Coutinho, E.S.F.; Barufaldi, L.A.; Abreu, G.D.A.; Malhão, T.A.; de Souza, C.P.R.; Araujo, D.V. The Costs of Overweight and Obesity-Related Diseases in the Brazilian Public Health System: Cross-Sectional Study. *BMC Public Health* **2012**, *12*, 440.
- Anderson, M.R.; Shashaty, M.G.S. Impact of Obesity in Critical Illness. *Chest* **2021**, *160*, 2135–2145. [[CrossRef](#)]
- Ibrahim, M.M. Subcutaneous and Visceral Adipose Tissue: Structural and Functional Differences. *Obes. Rev.* **2010**, *11*, 11–18. [[CrossRef](#)] [[PubMed](#)]
- Tang, L.; Zhang, F.; Tong, N. The Association of Visceral Adipose Tissue and Subcutaneous Adipose Tissue with Metabolic Risk Factors in a Large Population of Chinese Adults. *Clin. Endocrinol.* **2016**, *85*, 46–53. [[CrossRef](#)]
- Sun, Z.; Lee, S.H.; Gepner, B.D.; Rigby, J.; Hallman, J.J.; Kerrigan, J.R. Comparison of Porcine and Human Adipose Tissue Loading Responses under Dynamic Compression and Shear: A Pilot Study. *J. Mech. Behav. Biomed. Mater.* **2021**, *113*, 104112. [[CrossRef](#)] [[PubMed](#)]
- Sun, Z.; Gepner, B.; Lee, S.; Oyen, M.; Rigby, J.; Cottler, P.S.; Hallman, J.; Kerrigan, J. Effect of Temperature and Freezing On Human Adipose Tissue Material Properties Characterized by High-Rate Indentation-Puncture Testing. *J. Biomech. Eng.* **2021**, *144*, 034502-1–034502-6. [[CrossRef](#)] [[PubMed](#)]

21. Alkhouli, N.; Mansfield, J.; Green, E.; Bel, J.; Knight, B.; Liversedge, N.; Tham, J.C.; Welbourn, R.; Shore, A.C.; Kos, K.; et al. The Mechanical Properties of Human Adipose Tissues and Their Relationships to the Structure and Composition of the Extracellular Matrix. *Am. J. Physiol. Endocrinol. Metab.* **2013**, *305*, 1427–1435. [[CrossRef](#)]
22. Comley, K.; Fleck, N.A. A Micromechanical Model for the Young's Modulus of Adipose Tissue. *Int. J. Solids Struct.* **2010**, *47*, 2982–2990. [[CrossRef](#)]
23. Juliar, B.A.; Strieder-barboza, C.; Karmakar, M.; Flesher, C.G.; Baker, N.A.; Varban, O.A.; Lumeng, C.N.; Putnam, A.J.; Robert, W.; Rourke, O. Viscoelastic Characterization of Diabetic and Non-Diabetic Human Adipose Tissue. *Biorheology* **2021**, *57*, 15–26. [[CrossRef](#)]
24. Sun, Z.; Gepner, B.D.; Lee, S.H.; Rigby, J.; Cottler, P.S.; Hallman, J.J.; Kerrigan, J.R. Multidirectional Mechanical Properties and Constitutive Modeling of Human Adipose Tissue under Dynamic Loading. *Acta Biomater.* **2021**, *129*, 188–198. [[CrossRef](#)] [[PubMed](#)]
25. Geerligs, M.; Peters, G.W.M.; Ackermans, P.A.J.; Oomens, C.W.J.; Baaijens, F.P.T. Linear Viscoelastic Behavior of Subcutaneous Adipose Tissue. *Biorheology* **2008**, *45*, 677–688. [[CrossRef](#)] [[PubMed](#)]
26. Mihai, L.A.; Chin, L.K.; Janmey, P.A.; Goriely, A. A Comparison of Hyperelastic Constitutive Models Applicable to Brain and Fat Tissues. *J. R. Soc. Interface* **2015**, *12*, 20150486. [[CrossRef](#)]
27. Unamuno, X.; Gómez-Ambrosi, J.; Becerril, S.; Álvarez-Cienfuegos, F.J.; Ramírez, B.; Rodríguez, A.; Ezquerro, S.; Valentí, V.; Moncada, R.; Mentxaka, A.; et al. Changes in Mechanical Properties of Adipose Tissue after Bariatric Surgery Driven by Extracellular Matrix Remodelling and Neovascularization Are Associated with Metabolic Improvements. *Acta Biomater.* **2022**, *141*, 264–279. [[CrossRef](#)]
28. Lanzl, F.; Duddeck, F.; Willuweit, S.; Peldschus, S. Experimental Characterisation of Porcine Subcutaneous Adipose Tissue under Blunt Impact up to Irreversible Deformation. *Int. J. Legal Med.* **2022**, *136*, 897–910. [[CrossRef](#)]
29. Busetto, L.; Dicker, D.; Azran, C.; Batterham, R.L.; Farpour-Lambert, N.; Fried, M.; Hjelmæsæth, J.; Kinzl, J.; Leitner, D.R.; Makaronidis, J.M.; et al. Obesity Management Task Force of the European Association for the Study of Obesity Released “Practical Recommendations for the Post-Bariatric Surgery Medical Management”. *Obes. Surg.* **2018**, *28*, 2117–2121. [[CrossRef](#)]
30. Kueper, M.A.; Kramer, K.M.; Kirschniak, A.; Königsrainer, A.; Pointner, R.; Granderath, F.A. Laparoscopic Sleeve Gastrectomy: Standardized Technique of a Potential Stand-Alone Bariatric Procedure in Morbidly Obese Patients. *World J. Surg.* **2008**, *32*, 1462–1465. [[CrossRef](#)]
31. Hayes, K.; Eid, G. Laparoscopic Sleeve Gastrectomy: Surgical Technique and Perioperative Care. *Surg. Clin. N. Am.* **2016**, *96*, 763–771. [[CrossRef](#)]
32. Mazurkiewicz, A. The Effect of Trabecular Bone Storage Method on Its Elastic Properties. *Acta Bioeng. Biomech.* **2018**, *20*, 21–27. [[CrossRef](#)]
33. Fontanella, C.G.; Belluzzi, E.; Pozzuoli, A.; Favero, M.; Ruggieri, P.; Macchi, V.; Carniel, E.L. Mechanical Behavior of Infrapatellar Fat Pad of Patients Affected by Osteoarthritis. *J. Biomech.* **2022**, *131*, 110931. [[CrossRef](#)]
34. Carniel, E.L.; Albanese, A.; Fontanella, C.G.; Pavan, P.G.; Prevedello, L.; Salmaso, C.; Todros, S.; Toniolo, I.; Foletto, M. Biomechanics of Stomach Tissues and Structure in Patients with Obesity. *J. Mech. Behav. Biomed. Mater.* **2020**, *110*, 103883. [[CrossRef](#)] [[PubMed](#)]
35. Yang, W.; Fung, T.C.; Chian, K.S.; Chong, C.K. Viscoelasticity of Esophageal Tissue and Application of a QLV Model. *J. Biomech. Eng.* **2006**, *128*, 909–916. [[CrossRef](#)]
36. Screen, H.R.C.; Toorani, S.; Shelton, J.C. Microstructural Stress Relaxation Mechanics in Functionally Different Tendons. *Med. Eng. Phys.* **2013**, *35*, 96–102. [[CrossRef](#)] [[PubMed](#)]
37. Natali, A.N.; Carniel, E.L.; Frigo, A.; Fontanella, C.G.; Rubini, A.; Avital, Y.; De Benedictis, G.M. Experimental Investigation of the Structural Behavior of Equine Urethra. *Comput. Methods Programs Biomed.* **2017**, *141*, 35–41. [[CrossRef](#)] [[PubMed](#)]
38. Fallah, A.; Ahmadian, M.T.; Firozbakhsh, K.; Aghdam, M.M. Micromechanical Modeling of Rate-Dependent Behavior of Connective Tissues. *J. Theor. Biol.* **2017**, *416*, 119–128. [[CrossRef](#)] [[PubMed](#)]
39. Holzapfel, G.A.; Gasser, T.C.; Ogden, R.W. A New Constitutive Framework for Arterial Wall Mechanics and a Comparative Study of Material Models. *J. Elast.* **2000**, *61*, 1–48. [[CrossRef](#)]
40. Natali, A.N.; Fontanella, C.G.; Carniel, E.L. Constitutive Formulation and Numerical Analysis of the Heel Pad Region. *Comput Methods Biomech. Biomed. Eng.* **2012**, *15*, 401–409. [[CrossRef](#)]
41. Carniel, E.L.; Fontanella, C.G.; Stefanini, C.; Natali, A.N. A Procedure for the Computational Investigation of Stress-Relaxation Phenomena. *Mech. Time Depend. Mater.* **2013**, *17*, 25–38. [[CrossRef](#)]
42. Edwards, L.A.; Bugaresti, J.M.; Buchholz, A.C. Visceral Adipose Tissue and the Ratio of Visceral to Subcutaneous Adipose Tissue Are Greater in Adults with than in Those without Spinal Cord Injury, despite Matching Waist Circumferences. *Am. J. Clin. Nutr.* **2008**, *87*, 600–607. [[CrossRef](#)] [[PubMed](#)]
43. Pandey, A.; Kumar, P.; Aithal, K.; Sushma, R. Morphometry of Subcutaneous Fat Lobules of the Abdomen and Its Implication in Obesity. *Plast. Aesthet. Res.* **2015**, *2*, 286.
44. Lin, M.; Ge, J.; Wang, X.; Dong, Z.; Xing, M.; Lu, F.; He, Y. Biochemical and Biomechanical Comparisons of Decellularized Scaffolds Derived from Porcine Subcutaneous and Visceral Adipose Tissue. *J. Tissue Eng.* **2019**, *10*, 2041731419888168. [[CrossRef](#)]
45. Kim, M.; Lee, C.; Park, J. Extracellular Matrix Remodeling Facilitates Obesity-Associated Cancer Progression. *Trends Cell Biol.* **2022**; 1–10, in press. [[CrossRef](#)] [[PubMed](#)]

46. Sturm, R. Increases in Morbid Obesity in the USA: 2000–2005. *Public Health* **2007**, *121*, 492–496. [[CrossRef](#)]
47. Calvo-Gallego, J.L.; Domínguez, J.; Gómez Cía, T.; Gómez Ciriza, G.; Martínez-Reina, J. Comparison of Different Constitutive Models to Characterize the Viscoelastic Properties of Human Abdominal Adipose Tissue. A Pilot Study. *J. Mech. Behav. Biomed. Mater.* **2018**, *80*, 293–302. [[CrossRef](#)]
48. Naseri, H.; Johansson, H. A Priori Assessment of Adipose Tissue Mechanical Testing by Global Sensitivity Analysis. *J. Biomech. Eng.* **2018**, *140*, 051008-1–051008-10. [[CrossRef](#)]